

# Reflection high-energy positron diffraction study on Si(111)- $\sqrt{3} \times \sqrt{3}$ -Ag surface

Y. Fukaya\* and A. Kawasuso

Advanced Science Research Center, Japan Atomic Energy Agency, 1233 Watanuki, Takasaki, Gunma 370-1292, Japan

A. Ichimiya

Advanced Science Research Center, Japan Atomic Energy Agency, 1233 Watanuki, Takasaki, Gunma 370-1292, Japan

and Faculty of Science, Japan Women's University, 2-8-1 Mejirodai, Bunkyo-ku, Tokyo 112-8681, Japan

(Received 28 December 2006; published 27 March 2007)

We carried out a reflection high-energy positron diffraction study on a Si(111)- $\sqrt{3} \times \sqrt{3}$ -Ag surface at temperatures ranging from 50 to 800 K. We found that the rocking curves obtained both below and above the critical temperature of the phase transition ( $T_c$ ) can be explained with the inequivalent triangle (IET) model by introducing an order parameter between the IET(+) and IET(-) phases. We determined the length and rotation angle of the Ag triangle to be  $2.76 \pm 0.02$  Å and  $5.3 \pm 0.5^\circ$ , respectively. We also determined the surface parallel and normal Debye temperatures of the topmost Ag atoms to be 110 and 140 K, respectively. We found that the temperature dependence of the total reflection intensities below  $T_c$  can be completely reproduced by considering the order-disorder phase transition for a critical exponent of  $\beta$  given by  $0.28 \pm 0.05$ .

DOI: 10.1103/PhysRevB.75.115424

PACS number(s): 68.35.Rh, 61.14.Hg, 68.35.Bs

## I. INTRODUCTION

The Si(111)- $\sqrt{3} \times \sqrt{3}$ -Ag surface has been extensively studied as a typical two-dimensional metal-semiconductor system by using several surface techniques.<sup>1</sup> In 1988, after a long-lasting controversy, the honeycomb-chained-triangle (HCT) model [see Fig. 1(a)] was proposed as the structure of this surface at room temperature.<sup>2</sup> On the other hand, in 1999, the inequivalent triangle (IET) model [shown in Figs. 1(b) and 1(c)] was predicted as the ground-state structure from a first-principles-calculation study.<sup>3</sup> In the IET model, the topmost Ag atoms are slightly shifted by approximately 0.29 Å [upward for IET(+) in Fig. 1(b) and downward for IET(-) in Fig. 1(c)] as compared to the HCT model. Subsequently, the IET model was confirmed by low-temperature scanning tunneling microscopy (STM) studies.<sup>4</sup> These results indicate that the Si(111)- $\sqrt{3} \times \sqrt{3}$ -Ag surface undergoes a displacive phase transition for temperatures below room temperature. Indeed, surface x-ray diffraction (SXRD) and reflection high-energy electron diffraction (RHEED) studies have indicated that the displacive phase transition between the IET and HCT structures occurs at around 150 K.<sup>5,6</sup>

However, theoretical studies using Monte Carlo simulations suggest that an order-disorder phase transition occurs.<sup>7-9</sup> Thus, the high-temperature phase does not correspond to the HCT model but to a thermally fluctuating state between two topologically different IET sites, i.e., IET(+) and IET(-), as shown in Figs. 1(b) and 1(c). Recently, an angle-resolved photoemission spectroscopy study revealed that the band structure does not change below room temperature, suggesting the occurrence of an order-disorder phase transition.<sup>10</sup> We confirmed this occurrence by conducting a structural analysis using reflection high-energy positron diffraction (RHEPD).<sup>11</sup> A similar result was obtained by a photoelectron diffraction study.<sup>12</sup> More recently, it was shown that high-resolution STM images at both room temperature and low temperatures exhibit the IET structure.<sup>13</sup>

In this study, we performed a systematic RHEPD study on the Si(111)- $\sqrt{3} \times \sqrt{3}$ -Ag surface. One of the most important

advantages of RHEPD is the occurrence of total reflection.<sup>14,15</sup> In this technique, the diffraction intensities are very sensitive to the topmost surface structure and thermal vibration state, and hence we are able to study the topmost surfaces with negligible disturbance from the bulk.<sup>16,17</sup> We measured the rocking curves and temperature dependence of the RHEPD intensities for a wide range of temperatures. We report on the optimized structures and Debye temperatures of the Si(111)- $\sqrt{3} \times \sqrt{3}$ -Ag surface. Furthermore, we demonstrate the occurrence of the order-disorder phase transition.

## II. EXPERIMENT

The samples were cut from a mirror-polished *n*-type Si(111) wafer with a resistivity of 1–10 Ω cm. After clean-

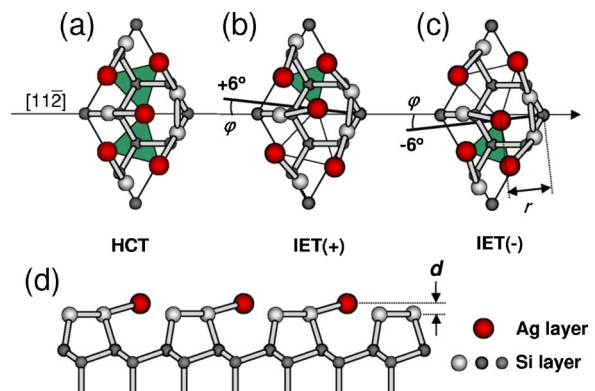


FIG. 1. (Color online) Schematic drawings of (a) honeycomb-chained-triangle (HCT) and two topologically different inequivalent triangle (IET) models, (b) IET(+) and (c) IET(-), for the Si(111)- $\sqrt{3} \times \sqrt{3}$ -Ag surface (top view). The rotation angles ( $\varphi$ ) of the Ag atoms for the IET(+) and IET(-) models are  $+6^\circ$  and  $-6^\circ$  on the basis of the HCT model, respectively. The side view of the structure model is displayed in (d).  $r$ ,  $\varphi$ , and  $d$  denote the cylindrical coordinates of the Ag atoms.

ing the samples with ethanol, they were transferred into a vacuum chamber evacuated with a base pressure of  $5 \times 10^{-8}$  Pa. Subsequently, they were heated at 673 K for several hours for degassing and flashed a few times at 1473 K for 10 s in order to obtain clean  $7 \times 7$  reconstructed surfaces. Finally, Ag atoms of one monolayer ( $7.8 \times 10^{14} \text{ cm}^{-2}$ ) were deposited onto the reconstructed surfaces at 773 K by using an electron-beam evaporator or alumina-coated tungsten basket. The substrate temperature was calibrated with an infrared radiation thermometer and thermocouple attached near the sample.

The positron beams were generated using sodium-22 sources, tungsten moderators, and electromagnetic or electrostatic lenses. Details of the apparatus were described elsewhere.<sup>18,19</sup> The energies of the positron beams ( $E$ ) were set at 10 or 20 keV. They were irradiated onto the sample surfaces, and diffracted beams were observed by using a micro channel plate assembly with a phosphor plane. During the measurement of the rocking curve, the glancing angle ( $\theta$ ) of the incident positron beam was varied by rotating the sample holder. The sample temperature was changed from 50 to 800 K by using a cryostat and resistive heating.

### III. RESULTS AND DISCUSSIONS

#### A. Surface structure

Figure 2 shows the RHEPD patterns observed for the Si(111)- $\sqrt{3} \times \sqrt{3}$ -Ag surface at 103 and 293 K ( $E=10$  keV). The fractional-order spots with the indices  $(1/3 \ 1/3)$  and  $(2/3 \ 2/3)$  that suggest the formation of  $\sqrt{3} \times \sqrt{3}$  periodicity are labeled. Although the pattern itself does not change with temperature, the intensity of the  $(1/3 \ 1/3)$  spot at 103 K is significantly strong as compared to that at 293 K. In Fig. 3, the circles show the rocking curves of the specular spots measured for the one-beam condition (the incident azimuth is  $7.5^\circ$  with regard to the  $[11\bar{2}]$  direction) at 110 and 293 K ( $E=10$  keV). It is observed that the rocking curves at 110 and 293 K are nearly identical. In Figs. 4 and 5, the circles show the rocking curves measured for the many-beam condition (the azimuth is  $1.5^\circ$  with respect to the  $[11\bar{2}]$  direction) at 110 and 293 K ( $E=10$  keV). The curves of the  $(0 \ 0)$  and  $(2/3 \ 2/3)$  spots exhibit no apparent temperature dependences. The intensity of the  $(1/3 \ 1/3)$  spot at around  $2.5^\circ$  at 110 K is approximately twice as large as that at 293 K. The drastic increase in the intensity of the  $(1/3 \ 1/3)$  spot at low temperatures is consistent with the temperature dependence of the RHEPD pattern (see Fig. 2). We carried out the structural analysis of the Si(111)- $\sqrt{3} \times \sqrt{3}$ -Ag surface by using the above rocking curves.

First, we determine the vertical position of the Ag layer from the underlying Si trimer layer (denoted by  $d$  in Fig. 1) in the one-beam condition. In this condition, the specular intensity depends on the interlayer distance and density of the surface layer because the simultaneous reflections in the plane are sufficiently suppressed.<sup>20</sup> By adjusting  $d$ , we determined the theoretical rocking curves based on the dynamical diffraction theory in order to reproduce the experimental

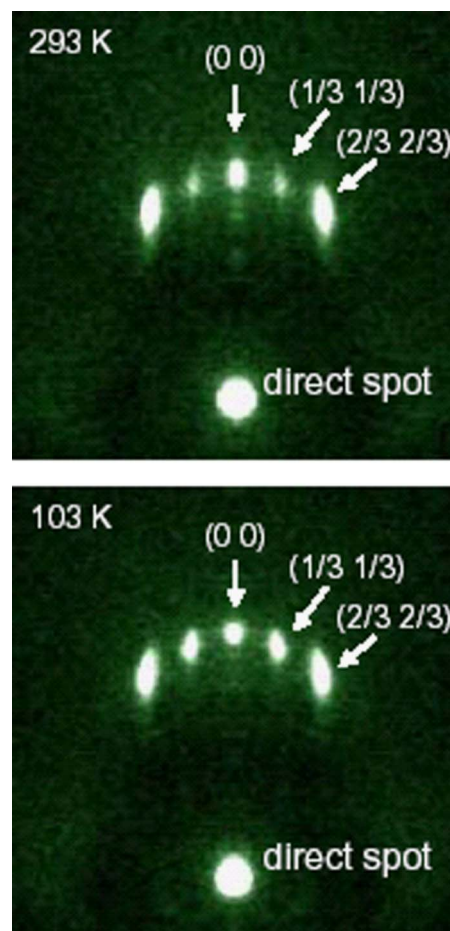


FIG. 2. (Color online) RHEPD patterns measured from the Si(111)- $\sqrt{3} \times \sqrt{3}$ -Ag surface at 293 K (upper panel) and at 103 K (bottom panel). The glancing angle and azimuth of the incident positrons are  $3.0^\circ$  and the  $[11\bar{2}]$  direction, respectively. The incident positron energy is 10 keV. The patterns are displayed by the superposition of the left and right parts.

curves.<sup>21</sup> In the calculation, the surface Debye temperatures of the Ag and Si atoms were assumed to be 140 and 610 K, respectively, as determined in the subsequent section. The absorption potentials for the Ag and Si atoms due to electronic excitations were assumed to be 0 and 1.7 V, respectively.<sup>22,23</sup> In Fig. 3, the solid lines show the curves that were determined. When  $d=0$  Å, which means that the Ag layer is situated at the Si trimer layer, a broad peak extending up to a glancing angle of  $4.5^\circ$  appears. This reflects the enhancement of the surface potential due to the superposition of the Ag layer and the underlying Si layer. As  $d$  increases, the positions of the total reflection peak and the  $(111)$  and  $(222)$  Bragg reflection peaks shift toward a lower angle. When  $d > 1$  Å, additional peaks appear on the shoulder of the large peak. Further, small dips appear around  $2.0^\circ$ – $2.5^\circ$ . Other peaks such as the  $(333)$  and  $(444)$  Bragg reflection peaks dramatically change with  $d$ . At both 110 and 293 K, the experimental curves are compatible with the calculated ones for  $d=0.5$ – $1.0$  Å. By minimizing the reliability factor  $R = \sqrt{\sum_{\theta} (I_{\theta}^{\text{expt}} - I_{\theta}^{\text{calc}})^2}$ , where  $\sum_{\theta} I_{\theta}^{\text{expt}} = \sum_{\theta} I_{\theta}^{\text{calc}} = 100\%$ ,<sup>17</sup> we obtained  $d=0.74$  Å at 110 K and  $d=0.78$  Å at 293 K.<sup>11</sup>

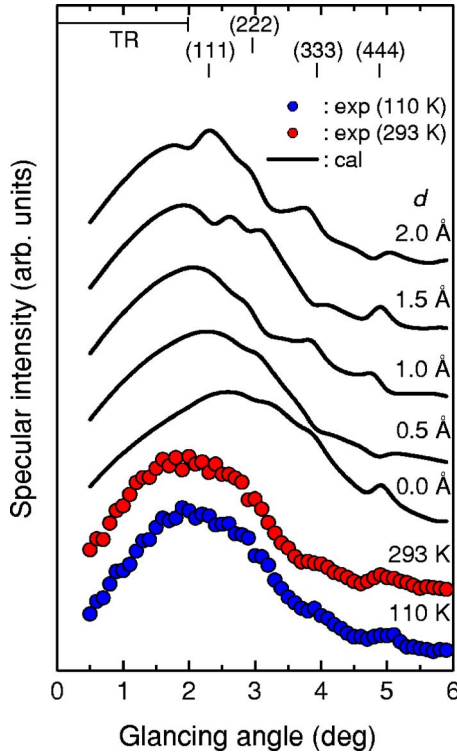


FIG. 3. (Color online) RHEPD rocking curves for the specular spot on the Si(111)- $\sqrt{3} \times \sqrt{3}$ -Ag surface under the one-beam condition. The incident positron energy is 10 keV. The blue and red circles denote the experimental curves at 110 and 293 K, respectively. The solid lines show the rocking curves that were calculated based on the dynamical diffraction theory by using various values of heights ( $d$ ) for the Ag triangle from the underlying Si trimer. “TR” stands for the total reflection region.

Next, we determine the lateral positions of the Ag atoms by using the rocking curves for the many-beam condition. Basically, by changing the length  $r$  of the Ag triangle and the rotation angle  $\varphi$ , as shown in Fig. 1, we determine the rocking curve in order to reproduce the experimental curves. However, not only these parameters but also another fitting parameter—order parameter  $p$ —is required, as described below. When  $\varphi \neq 0^\circ$ , the two domains composed of IET(+) and IET(-) phases coexist because of the absence of an energy difference. In each domain, their antiphases are also mixed. Assuming  $n_+$  and  $n_-$  to be the fraction of the IET(+) and IET(-) phases in one of the domains ( $n_+ + n_- = 1$ ), we can define  $p$  by the expression  $(n_+ - n_-)/(n_+ + n_-)$ . The diffraction intensity of this domain is given as a function of  $p$ , i.e.,  $I_{hk}(p)$ . The diffraction intensity for its antiphase domain is explicitly given by  $I_{hk}(-p)$ . Consequently, the total diffraction intensity is given by

$$I_{hk}^{\text{total}}(p) = I_{hk}(p) + I_{hk}(-p). \quad (1)$$

The dependence of  $I_{hk}$  on  $p$  is calculated from the dynamical diffraction theory. Figure 6(a) shows  $I_{hk}^{\text{total}}(p)$  calculated from the dynamical theories under the same condition as that in experiments (incident azimuth,  $1.5^\circ$  from the  $[11\bar{2}]$  direction; glancing angle,  $2.0^\circ$ ). The intensities of the (0 0) and

(2/3 2/3) spots have only a weak dependence on  $p$ . The intensity of the (1/3 1/3) spot dramatically changes with  $p$ . The above-mentioned behavior is well approximated by the parabolic function of  $p$ . Here, to understand the physical meaning of  $I_{hk}(p)$ , we briefly introduce the kinematical expression. The structure factor can be expressed by

$$F(p) = \frac{1+p}{2}F_+ + \frac{1-p}{2}F_-, \quad (2)$$

where  $F_+$  and  $F_-$  are the structure factors for the IET(+) and IET(-) phases, respectively. Generally, the structure factor is given by  $F = \sum_i f_i \exp(-ibx_i)$ , where  $f_i$  is an atomic scattering factor for the  $i$ th atom, and  $b$  and  $x_i$  are the scattering vector and atomic position, respectively. The total intensity is given by

$$I_{hk}^{\text{total}}(p) = |F(p)|^2 + |F(-p)|^2 = \frac{1+p^2}{2} \{|F_+|^2 + |F_-|^2\} + \frac{1-p^2}{2} \{F_+F_-^* + F_-F_+^*\} = 2 \text{Re}(F_+)^2 + 2p^2 \text{Im}(F_+)^2. \quad (3)$$

Here, we have used the relationship  $F_+ = F_-^*$  ( $F_- = F_+^*$ ) because of the symmetry of the atomic positions for the Ag atoms in the IET(+) and IET(-) structures. Figure 6(b) shows  $I_{hk}^{\text{total}}(p)$  calculated by the kinematical theory. The intensities of the (0 0) and (2/3 2/3) spots are nearly independent of  $p$ . The intensity of the (1/3 1/3) spot drastically changes with  $p$ . These features are in good agreement with those calculated by the dynamical theory. The reason for the weak dependence of the intensities of the (0 0) and (2/3 2/3) spots on  $p$  is due to the condition  $|\text{Re}(F_+)| > |\text{Im}(F_+)|$ . The strong dependence of the (1/3 1/3) spot intensity on  $p$  is due to the condition  $|\text{Re}(F_+)| \cong |\text{Im}(F_+)|$ . That is, the intensity due to the interference between the IET(+) and IET(-) phases is small as compared to the intensities of the (0 0) and (2/3 2/3) spots. On the other hand, the effect of the interference on the intensity becomes large for the (1/3 1/3) spot because the intensity from the single IET(+) or IET(-) domain is relatively small.

In Figs. 4(a)–4(c), the solid lines show the rocking curves determined for various values of  $p$  while retaining the values  $\varphi = 6^\circ$  and  $r = 2.82 \text{ \AA}$ . The rocking curves for the (0 0) spot do not show a drastic change with a variation in  $p$  although the intensity of the spot decreases with an increase in  $p$  [Fig. 4(a)]. The rocking curves of the (2/3 2/3) spot have a similar tendency [Fig. 4(c)]. On the other hand, the intensity of the rocking curve of the (1/3 1/3) spot increases with an increase in  $p$  [Fig. 4(b)]. By minimizing the reliability factor, we eventually obtained the values  $\varphi = 5.7^\circ$ ,  $r = 2.78 \text{ \AA}$ , and  $p = 0.4$  as the optimized values at 110 K. In the same way as mentioned above, we analyzed the rocking curves at 293 K. In Figs. 5(a)–5(c), the solid lines show the rocking curves calculated at various values of  $\varphi$  while retaining the values  $r = 2.82 \text{ \AA}$  and  $p = 0$ . The large total reflection peak for the (0 0) spot shifts to a higher angle with an increase in the rotation angle [Fig. 5(a)]. Moreover, the width of the peak

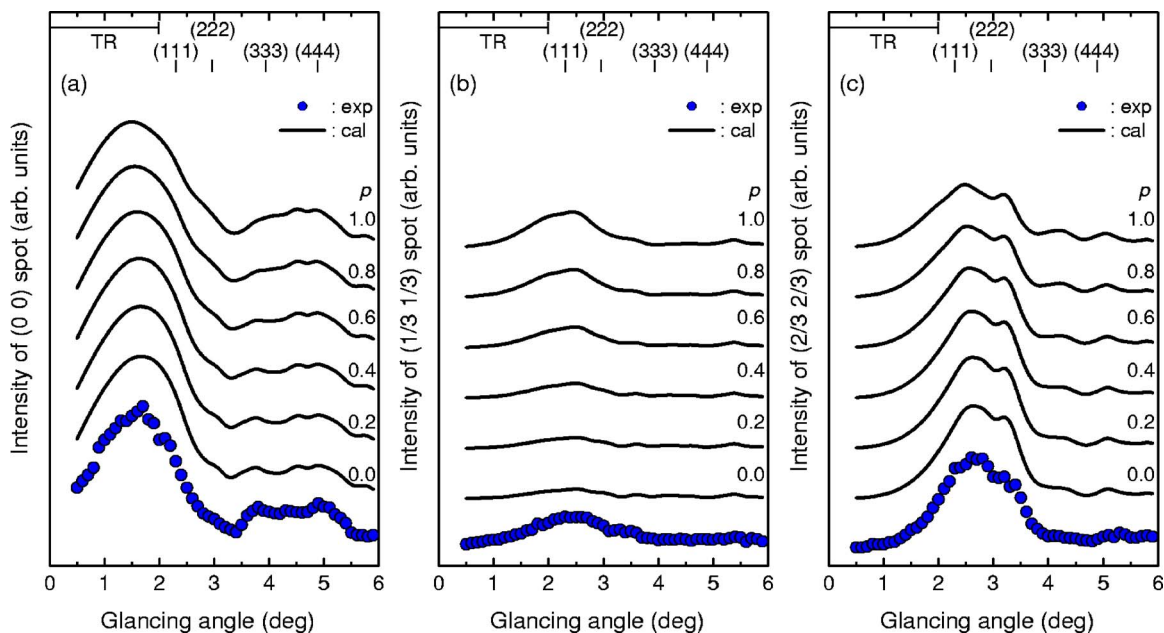


FIG. 4. (Color online) RHEPD rocking curves for the (a) (0 0) spot, (b) (1/3 1/3) spot, and (c) (2/3 2/3) spot on the Si(111)- $\sqrt{3} \times \sqrt{3}$ -Ag surface at 110 K. The incident positron energy is 10 keV. The circles indicate the measured intensities. The solid lines show the rocking curves determined using various values of  $p$  for the Ag atoms at the IET(+) and IET(-) sites.  $p$  indicates the order parameter between the IET(+) and IET(-) phases.

becomes larger with an increase in the rotation angle. Furthermore, small peaks at angles greater than  $\theta=3^\circ$  shift to higher angles with an increase in the rotation angle. As shown in Fig. 5(b), the rocking curve of the (1/3 1/3) spot does not change drastically because the intensity remains small for changing values of  $\varphi$ . In the curve for the (2/3 2/3) spot [Fig. 5(c)], the peaks shift to a higher angle with a decrease in the intensity when  $\varphi$  increases. By mini-

mizing the reliability factor, we eventually obtained  $\varphi=4.8^\circ$ ,  $r=2.74 \text{ \AA}$ , and  $p=0$  as the optimum values. The structure parameters are summarized in Table I.

Thus, the structure of the Si(111)- $\sqrt{3} \times \sqrt{3}$ -Ag surface is explained by the IET model at both temperatures of 110 and 293 K. The phase transition of this surface is known to take place at 120–150 K.<sup>5,6</sup> The above results show that none of the structure parameters ( $d$ ,  $\varphi$ , and  $r$ ) changes during the

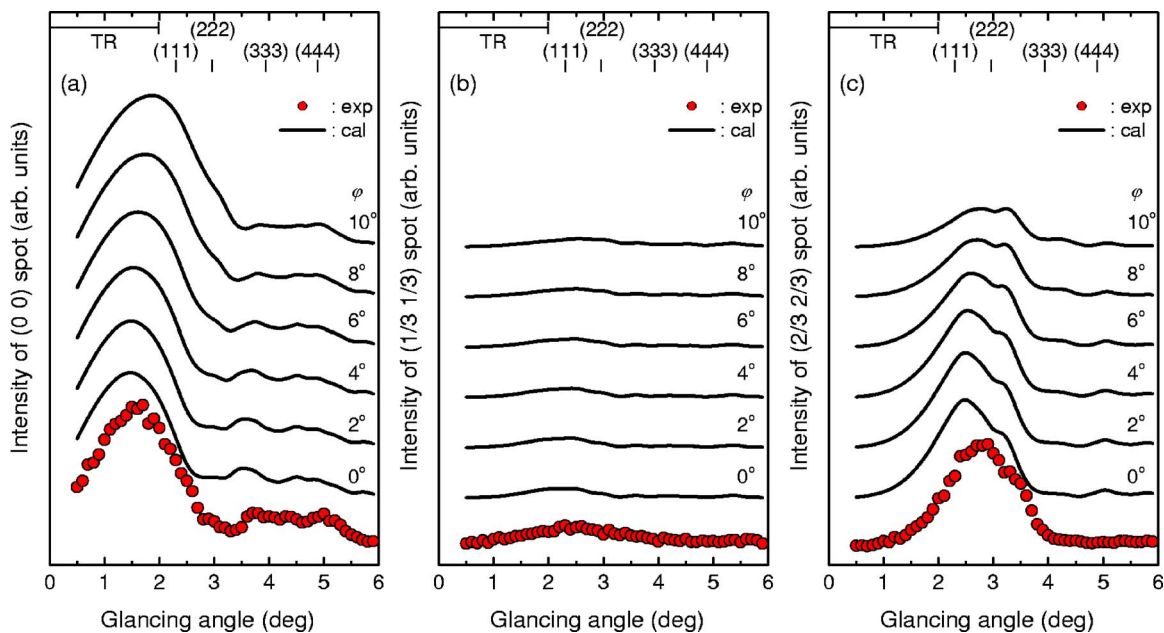


FIG. 5. (Color online) RHEPD rocking curves for the (a) (0 0) spot, (b) (1/3 1/3) spot, and (c) (2/3 2/3) spot on the Si(111)- $\sqrt{3} \times \sqrt{3}$ -Ag surface at 293 K. The incident positron energy is 10 keV. The circles denote the measured intensities. The solid lines show the rocking curves determined by using various rotation angles ( $\varphi$ ) for the Ag triangle with regard to the HCT structure.

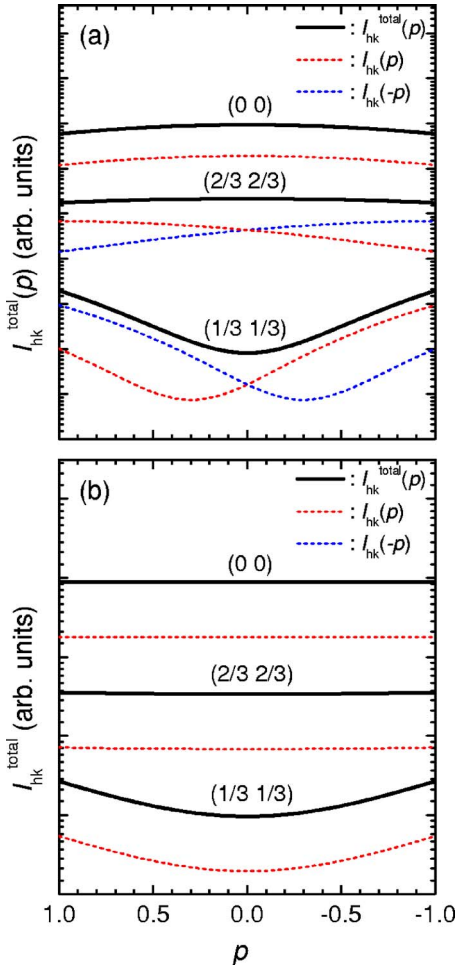


FIG. 6. (Color online) Calculated RHEPD intensities for the (0 0), (1/3 1/3), and (2/3 2/3) spots on the Si(111)- $\sqrt{3} \times \sqrt{3}$ -Ag surface as a function of  $p$  for the Ag atoms at the IET(+) and IET(-) sites. The intensities are calculated based on (a) dynamical and (b) kinematical diffraction theories. The incident condition is the same as that in Fig. 4.

phase transition. Therefore, it is concluded that a displacive phase transition does not occur. Only  $p$  changes with the temperature. We show the possibility of an order-disorder phase transition in the last subsection.

### B. Surface Debye temperature

We determined the Debye temperature of the Ag layer from the analyses of the temperature dependent spot intensi-

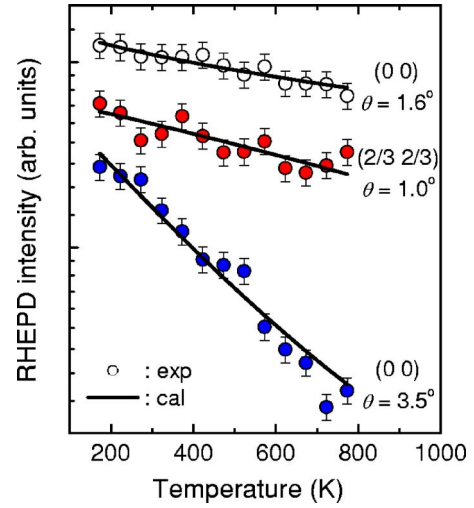


FIG. 7. (Color online) Temperature dependences of the RHEPD intensities for the (0 0) spot at  $\theta=1.6^\circ$  and  $\theta=3.5^\circ$  under the one-beam condition and for the (2/3 2/3) spot at  $\theta=1.0^\circ$  along  $1.5^\circ$  with regard to the  $[11\bar{2}]$  direction. The solid lines show the intensities calculated by using the Debye temperatures of 110 K (surface parallel) and 140 K (surface normal) for the topmost Ag atoms and the bulk Debye temperature of 610 K for the bulk Si atoms. The incident positron energy is 20 keV.

ties ( $E=20$  keV), as shown in Fig. 7. From the intensity slope of the (0 0) spot at  $\theta=1.6^\circ$  under the one-beam condition, we determined the normal component of the Debye temperature ( $\Theta_{\perp}^{\text{Ag}}$ ). Since a side spot such as the (2/3 2/3) spot has a large scattering vector parallel to the surface, we determined the parallel component of the Debye temperature ( $\Theta_{\parallel}^{\text{Ag}}$ ) from its intensity slope. Finally, we determined the Debye temperature ( $\Theta^{\text{Si}}$ ) of the Si layer from the intensity slope at the high glancing angles. The details are described elsewhere.<sup>17</sup> In Fig. 7, the solid lines represent the best temperature dependences of the spot intensities calculated by using the dynamical diffraction theory along with the optimized structure described in the preceding subsection. We obtained  $\Theta_{\perp}^{\text{Ag}}=140$  K,  $\Theta_{\parallel}^{\text{Ag}}=110$  K, and  $\Theta^{\text{Si}}=610$  K. Consequently, the parallel component is larger than the normal one, and hence the thermal vibration of Ag atoms is slightly anisotropic. The bulk Debye temperature for the Si(111)- $7 \times 7$  surface is consistent with that of the bulk atoms.<sup>17</sup> The anisotropy has also been obtained from a RHEED intensity analysis.<sup>24</sup> The root-mean-square amplitudes ( $\sqrt{\langle u^2 \rangle}$ ) of the Ag atoms are estimated to be 0.14 Å for the normal component and 0.18 Å for the parallel component at room tempera-

TABLE I. Structure parameters for the Si(111)- $\sqrt{3} \times \sqrt{3}$ -Ag surface.

	$T < T_c$			$T > T_c$			$\Theta_{\parallel}^{\text{Ag}}$ (K)	$\Theta_{\perp}^{\text{Ag}}$ (K)	$\beta$
	$r$ (Å)	$\varphi$	$d$	$r$ (Å)	$\varphi$	$d$			
This study	$2.78 \pm 0.09$	$5.7^\circ \pm 1.4^\circ$	$0.74 \text{ \AA} (110 \text{ K})$	$2.74 \pm 0.08$	$4.8^\circ \pm 1.3^\circ$	$0.78 \text{ \AA} (293 \text{ K})$	110	140	$0.28 \pm 0.05$
SXRD (Ref. 5)	$2.85 \pm 0.01$	$5.1^\circ (50 \text{ K})$		$2.85 \pm 0.01$	$0.0 (293 \text{ K})$		90		$0.27 \pm 0.03$
Theory (Refs. 3 and 8)	2.82	$6.0^\circ$					90		

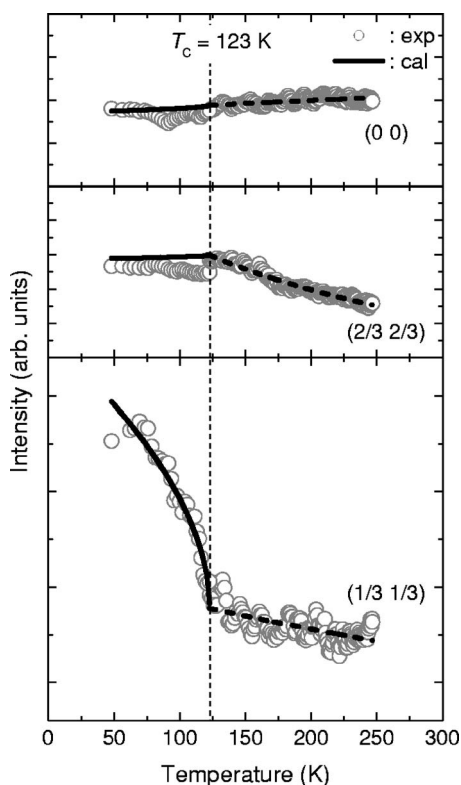


FIG. 8. Temperature dependence of the totally reflected RHEPD intensities for the (0 0), (1/3 1/3), and (2/3 2/3) spots on the Si(111)- $\sqrt{3} \times \sqrt{3}$ -Ag surface. The glancing angle is  $2.0^\circ$ , which satisfies the total reflection condition. The azimuthal angle corresponds to  $1.5^\circ$  with regard to the  $[11\bar{2}]$  direction. The incident positron energy is 10 keV. The circles denote the experimental intensities. The solid line shows the intensity calculated on the basis of the dynamical diffraction theory using the critical exponent of 0.28.

ture by using the above Debye temperatures. The value for the latter is comparable to those determined by Tajiri *et al.*<sup>5</sup> using the SXRD and by Kakitani *et al.*<sup>8</sup> by means of the Monte Carlo simulations.

### C. Phase transition

As shown in Sec. III A, the difference in the rocking curves below and above the phase-transition temperature can be explained by the change in the order parameter  $p$  between the IET(+) and IET(-) phases. Thus,  $p$  is recognized as the order parameter of the order-disorder phase transition. In order to confirm that the phase transition can be described in this way, we measured the temperature dependences of the

RHEPD intensities. Figure 8 shows the intensities of the individual spots ( $E=10$  keV) as a function of the temperature under the total reflection condition (the azimuthal angle was set as  $1.5^\circ$  with regard to the  $[11\bar{2}]$  direction). From the abrupt change in the intensities, we can specify the critical temperature of the phase transition ( $T_c$ ) as 123 K. The intensities of the (0 0) and (2/3 2/3) spots gradually decrease below  $T_c$ . On the other hand, the intensity of the (1/3 1/3) spot steeply increases below  $T_c$ . The order parameter is related to the critical exponent ( $\beta$ ) and  $T_c$  as follows:

$$p \propto \left| 1 - \frac{T}{T_c} \right|^\beta. \quad (4)$$

By varying  $\beta$ , we calculated the diffraction intensities based on the dynamical theory in order to reproduce the experimental temperature dependence below  $T_c$ . In Fig. 8, the solid lines show the optimum temperature dependences. Therefore, it is observed that the inferred temperature dependences are reasonably explained. The integrated intensity of a rocking curve in RHEED is abruptly changed at around 150 K,<sup>6</sup> which is not in contradiction to our result. The temperature dependence in RHEED should be explained by introducing the order parameter between the IET(+) and IET(-) phases. Finally, we obtained  $\beta=0.28 \pm 0.05$ . This is in good agreement with that obtained by SXRD.<sup>5</sup>

It is known that  $\beta=0.5$  for the mean-field approximation and  $\beta=0.125$  for the two-dimensional Ising model. For instance, in the case of Si(001), the critical exponent  $\beta$  corresponds to that of the two-dimensional Ising model.<sup>25</sup> The value of  $\beta$  in this case lies between the above-mentioned values and close to that expected for the three-dimensional Ising model ( $\beta \sim 0.325$ ). This implies that the interaction between the Ag and the Si atoms may have to be considered in the phase transition.

### IV. CONCLUSION

In this study, we studied the Si(111)- $\sqrt{3} \times \sqrt{3}$ -Ag surface using RHEPD. From the analyses of the rocking curves, we confirmed that the IET model is suitable for this surface both below and above  $T_c$ . We found that at a temperature  $T > T_c$ , the temperature dependences of the diffraction spot intensities are simply described by considering the surface Debye temperature, whereas at  $T < T_c$ , they are well explained by the order-disorder phase transition of the IET structure by introducing the order parameter between the IET(+) and IET(-) phases as the order parameter. From the critical exponent, it was inferred that the phase transition is described as being intermediate between the two-dimensional Ising model and the mean-field approximation.

\*Electronic address: fukaya.yuki99@jaea.go.jp

<sup>1</sup>S. Hasegawa, J. Phys.: Condens. Matter **12**, 463 (2000).

<sup>2</sup>T. Takahashi, S. Nakatani, N. Okamoto, T. Ishikawa, and S. Kikuta, Jpn. J. Appl. Phys., Part 2 **27**, L753 (1988).

<sup>3</sup>H. Aizawa, M. Tsukada, N. Sato, and S. Hasegawa, Surf. Sci.

**429**, L509 (1999).

<sup>4</sup>N. Sato, T. Nagao, and S. Hasegawa, Surf. Sci. **442**, 65 (1999).

<sup>5</sup>H. Tajiri, K. Sumitani, S. Nakatani, A. Nojima, T. Takahashi, K. Akimoto, H. Sugiyama, X. Zhang, and H. Kawata, Phys. Rev. B **68**, 035330 (2003).

- <sup>6</sup>H. Nakahara, T. Suzuki, and A. Ichimiya, *Appl. Surf. Sci.* **234**, 292 (2004).
- <sup>7</sup>N. Sasaki, S. Watanabe, H. Aizawa, and M. Tsukada, *Surf. Sci.* **493**, 188 (2001).
- <sup>8</sup>K. Kakitani, A. Yoshimori, H. Aizawa, and M. Tsukada, *Surf. Sci.* **493**, 200 (2001).
- <sup>9</sup>Y. Nakamura, Y. Kondo, J. Nakamura, and S. Watanabe, *Surf. Sci.* **493**, 206 (2001).
- <sup>10</sup>I. Matsuda, H. Morikawa, C. Liu, S. Ohuchi, S. Hasegawa, T. Okuda, T. Kinoshita, C. Ottaviani, A. Cricenti, M. D'angelo P. Soukiassian, and G. Le Lay, *Phys. Rev. B* **68**, 085407 (2003).
- <sup>11</sup>Y. Fukaya, A. Kawasuso, and A. Ichimiya, *e-J. Surf. Sci. Nanotechnol.* **3**, 228 (2005).
- <sup>12</sup>K. Sakamoto, T. Suzuki, K. Mawatari, K. Kobayashi, J. Okabayashi, K. Ono, N. Ueno, and M. Oshima, *Phys. Rev. B* **73**, 193303 (2006).
- <sup>13</sup>H. M. Zhang, J. B. Gustafsson, and L. S. O. Johansson, *Phys. Rev. B* **74**, 201304(R) (2006).
- <sup>14</sup>A. Kawasuso and S. Okada, *Phys. Rev. Lett.* **81**, 2695 (1998).
- <sup>15</sup>A. Ichimiya, *Solid State Phenom.* **28-29**, 143 (1992).
- <sup>16</sup>A. Kawasuso, Y. Fukaya, K. Hayashi, M. Maekawa, S. Okada, and A. Ichimiya, *Phys. Rev. B* **68**, 241313(R) (2003).
- <sup>17</sup>Y. Fukaya, A. Kawasuso, K. Hayashi, and A. Ichimiya, *Phys. Rev. B* **70**, 245422 (2004).
- <sup>18</sup>T. Ishimoto, A. Kawasuso, and H. Itoh, *Appl. Surf. Sci.* **194**, 43 (2002).
- <sup>19</sup>A. Kawasuso, T. Ishimoto, M. Maekawa, Y. Fukaya, K. Hayashi, and A. Ichimiya, *Rev. Sci. Instrum.* **75**, 4585 (2004).
- <sup>20</sup>A. Ichimiya, *Surf. Sci.* **192**, L893 (1987).
- <sup>21</sup>A. Ichimiya, *Jpn. J. Appl. Phys., Part 1* **22**, 176 (1983).
- <sup>22</sup>Y. Fukaya, A. Kawasuso, K. Hayashi, and A. Ichimiya, *Appl. Surf. Sci.* **244**, 166 (2005).
- <sup>23</sup>G. Radi, *Acta Crystallogr., Sect. A: Cryst. Phys., Diffr., Theor. Gen. Crystallogr.* **26**, 41 (1970).
- <sup>24</sup>M. Hashimoto, S. N. Takeda, and H. Daimon, *Phys. Rev. B* **71**, 113314 (2005).
- <sup>25</sup>T. Tabata, T. Aruga, and Y. Murata, *Surf. Sci.* **179**, L63 (1987).